

Near-Infrared Spectral Classification of late-M and L Dwarfs

I. Neill Reid

Dept. of Physics & Astronomy, University of Pennsylvania, 209 S. 33rd Street,
Philadelphia, PA 19104-6396; e-mail: inr@herschel.physics.upenn.edu

A. J. Burgasser

Dept. of Physics, 103-33, California Institute of Technology, Pasadena, CA 91125

K. L. Cruz

Dept. of Physics & Astronomy, University of Pennsylvania, 209 S. 33rd Street,
Philadelphia, PA 19104-6396

J. Davy Kirkpatrick

Infrared Processing and Analysis Center, 100-22, California Institute of Technology,
Pasadena, CA 91125

J. E. Gizis

Department of Physics and Astronomy, University of Massachusetts, Amherst, MA 01003

ABSTRACT

We present near-infrared (1 to 2.5 μm) low-resolution spectroscopy of eleven ultracool dwarfs with spectral types ranging from M7 to L8. Combining our observations with data published previously by Leggett *et al.* (2001), we have measured equivalent widths for the strongest atomic features and constructed narrowband indices to gauge the strength of the strongest molecular features. Those measurements show that the behaviour at near-infrared wavelengths is well correlated with spectral type, where the latter is defined from observations between 6300 and 10000 \AA . In particular, four indices designed to measure absorption in the wings of the 1.4 and 1.85 μm steam bands exhibit a linear, monotonic correlation with spectral type on the Kirkpatrick *et al.* (1999) system, allowing consistent calibration from both optical and near-infrared spectroscopy.

Subject headings: stars: low-mass, brown dwarfs – stars: late-type

1. Introduction

Spectral classification has played a vital role in astronomical research for almost 140 years. Originating with Secchi's (1866) division of the brightest stars into Classes I (Sirius-like), II (Sun-like) and III (Betelgeuse-like), the search for pattern and order has been crucial in understanding stellar structure and evolution. The classic Harvard system was developed by Fleming, Maury and Pickering in the 1890s, re-organised and refined by Cannon in the 1900s, and codified by Morgan, Keenan & Kellman in the 1940s (Morgan *et al.*, 1943). Boeshaar (1976) and Kirkpatrick, Henry & McCarthy (1991) extended calibration to spectral type M9.5. Yet, for all these additions, the basic scheme remained the Harvard system, running through OBAFGKM along the main sequence. That classification proved sufficient until the last few years of the twentieth century, when observations finally outstripped the system.

Spectral class M is characterised by the presence of TiO absorption. The advent of deep, wide-field near-infrared sky surveys catalysed both the discovery of numerous ultracool dwarfs with weak or no TiO absorption, and the creation of two new spectral types: class L, prototype GD 165B (Becklin & Zuckerman, 1988; Kirkpatrick, Henry & Liebert, 1993), characterised by metal-hydride bands and strong alkali lines; and class T, prototype Gl 229B (Nakajima *et al.*, 1995), characterised by methane absorption at 1.6 and 2.1 μm . Extensive follow-up optical spectroscopy has led to the definition of sub-types, L0 to L8, for the former class (Kirkpatrick *et al.*, 1999 - hereinafter, K99). At present, classification rests on molecular bandstrengths in the far red, between 0.6 and 1.0 μm , and acquiring spectra of adequate signal-to-noise at those wavelengths is a time consuming process for even the brightest L dwarfs. This technical problem can be circumvented to a large extent by calibrating the classification system at near-infrared wavelengths, where these cool dwarfs are significantly brighter. That issue is addressed in the current paper.

We have obtained intermediate resolution 0.9 to 2.5 μm spectra of a small sample of ultracool dwarfs with spectral types between M8 and L8. Our aim is the identification of suitable spectral-type indicators at those wavelengths, combining our own spectra with similar data from the literature, notably Leggett *et al.*'s (2001 - hereinafter, L2001) recent observations. We use these observations to confirm that variations in the more prominent near-infrared features preserve, by and large, the L0, L1...L8 sequence defined from optical spectroscopy. Rather than define an independent infrared classification system, we provide calibrating relations, based on the depth of the 1.4 and 1.85 μm steam bands, which transfer the Kirkpatrick *et al.* far-red system to near-infrared wavelengths. Section 2 describes the acquisition, reduction and calibration of our near-infrared spectra; section 3 discusses the photometric and spectroscopic properties of late-M and L dwarfs, and identifies

spectrophotometric indices suitable for spectral classification; and section 4 summarises our conclusions.

2. Observations

2.1. Data acquisition

Our observations were obtained on 19-22 December 1998 (UT) using the cooled grating spectrograph CGS4, mounted on the UK Infrared Telescope. Some cirrus was present during parts of the last two nights of the run, but seeing conditions were 1 arcsecond or better throughout. We used a 1.2 arcsecond slit, matched to 1 pixel on the detector, a 256×256 InSb array. We employed the 40 l/mm grating with the 150 mm camera to cover the near-infrared JHK régime in four settings: second order, centred at 1.10 and 1.35 μm , giving a resolution of 18 \AA or 550 kms^{-1} (designated J1 and J2); and first order, centred at 1.75 and 2.25 μm , at resolution $1,100 \text{ kms}^{-1}$ (designated H and K). The full spectral range covered by the four passbands is ~ 0.95 to $2.6 \mu\text{m}$, although terrestrial CO₂ absorption affects wavelengths beyond 2.5 μm .

We observed eleven ultracool dwarfs, ranging in spectral type from M7 to L8. Table 1 lists the targets and the journal of observations. The observations were made using a 2×2 sampling grid to minimise the effect of bad pixels, with individual (single frame) exposure times of 20 seconds at H and K and 30 seconds at J1 and J2. Flat-field exposures were obtained immediately preceding each programme star observation. Primary wavelength calibration is provided by xenon and krypton arc lamps. Each observation consisted of a series of paired exposures, nodding the telescope to move the star along the slit to permit accurate sky subtraction. The programme star observations, filter by filter, were interspersed with observations of bright F-type stars at small angular separation. Those stars serve to calibrate both absorption due to the terrestrial atmosphere and the overall energy distribution. The relevant reference stars for each source are listed in Table 1.

2.2. Data reduction

The successive pair-subtracted observations were combined using standard UKIRT programs to give a single image in each filter, with adjacent positive and negative summed spectra. Those spectra, together with the relevant reference star and arc-lamp spectra, were extracted using standard techniques implemented in the *iraf* reduction package. All of the stellar spectra were set on a wavelength scale and the individual observations of each source

combined.

The reference stars are mid-type F dwarfs, generally featureless at near-infrared wavelengths save for relatively narrow lines in the hydrogen Paschen and Brackett series. Eliminating those lines from the normalised spectra provides templates which can be used to correct for terrestrial absorption features in program objects observed at similar altitude and azimuth. The spectra can also be set on a relative flux scale, since the energy distribution of the high-temperature reference stars is well represented by a blackbody distribution. There is sufficient overlap between each of the four passbands employed here to allow accurate cross-calibration, permitting us to combine the data to form a single spectrum, covering 0.95 to 2.6 μm .

The flux zeropoint can be determined using broadband photometry, integrating the spectrum to determine the total flux encompassed within the 2MASS JHK_S passbands (f_J , f_H , f_{K_S} erg cm⁻² sec⁻¹). Since our spectra are on a relative flux scale, this is a two-step process: determining f_J , f_H and f_{K_S} at magnitude 0; and, given the appropriate conversion factors, scaling our spectra to match the broadband photometry listed in Table 1. We have determined the flux/magnitude conversion factors by applying our analysis to the L2001 observations of 2M0345. This ensures that, as far as possible, both sets of observations are tied to the same zeropoint. Note that we employ a single scaling factor for each composite spectrum, averaging the results from the J, H and K passbands, rather than adjusting each segment separately. In general, the magnitudes synthesised from the calibrated spectrophotometry agree with the broadband data to within 3-4%. The exceptions are the L2 dwarf, 2M1029, and the L7.5 dwarf, 2M0825; in both cases, the synthesised H and K magnitudes differ by +0.1 and -0.1 magnitudes, respectively, from the broadband measurements. These discrepancies are not important for present purposes.

Figures 1 and 2 plot the final calibrated spectra, where we use our optical spectroscopy to extend coverage to 6300Å. All of the latter observations except the data for LP 475-855 were obtained as part of our Keck 2MASS follow-up program using LRIS (Oke *et al.*, 1995), and the flux-calibrated spectra span 6300-10100Å at a resolution of 9 Å. Full details of the reduction and analysis are given by Kirkpatrick *et al.* (1999, 2000). The Keck optical spectra overlap with UKIRT J1 observations, providing an independent check on the photometrically-defined flux zeropoints. LP 475-855 was observed using the modular spectrograph on the Du Pont 100-inch telescope at Las Campanas observatory. This spectrum covers the wavelength range 6000 to 9500Å at a resolution of 12 Å. Our observation happened to catch the star during a flare outburst, which accounts for the strong (44Å equivalent width) H α emission.

Two of the L dwarfs included in our sample, 2M0345 and Denis0205, were also observed

at near-infrared wavelengths by Leggett *et al.* (2001). The L2001 data were also obtained with CGS4, using a nearly identical configuration to our own observations. There are, however, differences in the broadband photometry adopted for each dwarf, notably in the J-band: UKIRT photometry gives values of $J=13.92$ for 2M0345 and $J=14.43$ for Denis 0205; the corresponding 2MASS data are $J=14.03$ and $J=14.55$. This at least partly reflects differences in the transmission function of the respective J filters (note, however, that Dahn *et al.* (2000) find $J=14.59$ for Denis 0205 from USNO observations). The 2MASS and L2001 H and K photometry are in closer agreement. We use the 2MASS observations and transmission curves to calibrate our data.

Figure 3 compares the calibrated spectra. There is good agreement at most wavelengths in the case of the L0 dwarf, 2M0345, with the exception of the the 1.0 to $1.1\mu\text{m}$ region. The L2001 optical data, from Kirkpatrick, Beichman & Skrutskie (1997), are in good agreement with our Keck data. The Denis 0205 observations are more discrepant, notably between 0.85 and $1.05\mu\text{m}$ and beyond $2.35\mu\text{m}$. At longer wavelengths, our data are flatter than the L2001 observations. Our observations of 2M0825 also flatten in the 2.3 to $2.4\mu\text{m}$ range, but the L8 dwarf, 2M0310, has a steeper energy distribution.

Considering the discrepancy at shorter wavelengths, the L2001 optical data are from Tinney *et al.* (1998), with the flux zeropoint set by scaling the observations to match photometry in the $0.8\mu\text{m}$ I-band and $\sim 1\mu\text{m}$ z-band (Leggett, priv. comm.). In contrast, all our optical spectroscopy is calibrated directly against spectrophotometric standards. The two datasets are in good agreement for $\lambda < 0.8\mu\text{m}$, suggesting that the discrepancy may lie in the L2001 scaling to the z-band photometry. Our optical spectrum of Denis 0205 exhibits no anomalies when compared with our extensive observations of other L dwarfs, and we have no reason to doubt its reliability. Fortunately, neither of the long wavelength nor $1\mu\text{m}$ discrepancies is significant for the present analysis. However, we use limited wavelength coverage in constructing spectroscopic indices to minimise the effect of any residual flux-calibration uncertainties.

3. Infrared spectra and spectral classification

Spectral types serve as a form of astronomical shorthand notation, communicating in simple terms the overall appearance of a complex energy distribution. The emergent spectrum depends on the underlying stellar physics, and the expectation is that variations in spectral type reflect corresponding changes in significant physical parameters, notably effective temperature. A key tenet of any classification scheme must be that it rests solely on spectral morphology, independent of properties inferred from theoretical models. Spectral

types are defined by the relative strengths of specific atomic and molecular features - what the spectrum looks like. Relating those observed characteristics to physical parameters such as temperature, chemical abundance and gravity - what the star *is* - is a separate, and subsequent, operation. A classification system tied directly to physical parameters must continuously reinvent itself to follow the twists and turns of the latest theoretical models, and is therefore of limited value.

On the other hand, a spectral classification system should also be practical. The L dwarf spectral sequence, L0 to L8, has been defined using intermediate-resolution spectroscopy between 6300 to 10100 Å (K99)¹ Few L dwarfs have magnitudes brighter than I=19, making it difficult to obtain high signal-to-noise optical observations except with the largest available telescopes. In contrast, the much higher flux levels in the 1 to 2.5 μ m range render these dwarfs more accessible to spectroscopy at those wavelengths. Indeed, since the bulk of energy emitted by these cool dwarfs emerges at near-infrared wavelengths, it is important to ensure that the optically-defined spectral classification scheme currently in place orders L dwarfs in a manner consistent with the behaviour at 1 to 2.5 μ m.

Previous spectroscopy, notably by Jones *et al.* (1996), Viti & Jones (1999) and McLean *et al.* (2000), shows that late M and L dwarfs possess an array of near-infrared atomic lines and molecular bands, suitable for spectral classification. The strongest of those features are discussed further in the following section, where we show that the behavioural trends are compatible with variation in the optical spectral type. Given this consistency, there is no requirement to define an independent near-infrared spectral classification system. Combining the present sample with the late-type dwarfs observed by L2001 gives a total of eighteen dwarfs with spectral types of M8 or later, all with optically-determined spectral types; those ultracool dwarfs provide an excellent means of defining an infrared classification scheme which is tied to the established K99 L dwarf spectral sequence.

3.1. Photometric properties

Table 2 lists the available IJHK photometry for the sample of ultracool dwarfs considered here. Where possible, we list JHK observations from the USNO program (Dahn *et al.*, 2000), since those data are closer to the UKIRT system used by L2001. As noted

¹Martín *et al.* (1999) have defined an alternative classification scheme, tied directly to a temperature scale predicted by a specific set of theoretical models. This *modus operandi*, together with the fact that objects with morphologically distinct appearances can be classified as the same spectral type, disqualifies their scheme, in our view.

above, there can be differences of up to 0.1 magnitude with respect to the 2MASS data listed in Table 1, particularly in the J band. Twelve sources have accurate trigonometric parallax measurements, primarily from Dahn *et al.* (2000), and those data are also listed.

Figures 4 and 5 place these measurements in the broader context, plotting the $(M_J, (I-J))$ colour-magnitude diagram, and the far-red/near-infrared colour-colour and spectral-type/colour relations outlined by nearby stars and brown dwarfs. Our targets lie within the late-M/L-dwarf distribution in most of these diagrams; the exception is the (spectral type, $(J-K_s)$) relation, where the L3 to L7 dwarfs are among the bluer objects in their respective classes. This holds regardless of whether we use exclusively 2MASS photometry or the data listed in Table 2.

We have integrated the spectral energy distributions to determine bolometric magnitudes for the dwarfs in our sample. Following L2001, we allow for short wavelength radiation by linearly extrapolating from our shortest wavelength datum to $F_\lambda = 0$ at $\lambda = 0$; at long wavelengths, we assume that the flux distribution follows a Rayleigh-Jeans distribution. Between 65 and 75% of the total energy radiated by these ultracool dwarfs emerges between 1 and $2.5\mu\text{m}$; as L2001 emphasise, longer wavelengths account for most of the remainder.

Table 2 lists the bolometric corrections calculated for the J-band, where we also give the values derived from L2001. These results are plotted against spectral type in the lowest panel of Figure 5. As previously suggested (Reid *et al.*, 2000), there is relatively little variation in the J-band bolometric corrections of dwarfs cooler than Wolf 359 (spectral type M6); indeed, most of the dwarfs considered here have values of BC_J within 0.5 magnitudes of Leggett *et al.*'s (1999) result for Gl 229B. This relatively small spread in bolometric correction is in contrast to behaviour in the H and K passbands, where the onset of methane absorption leads to changes exceeding 1.5 magnitudes. M_J can therefore provide a good guide to total luminosity even in the absence of detailed spectroscopic information. The implications of these results for the likely temperature scale of the L dwarf sequence will be discussed in conjunction with near-infrared observations of a larger sample of L dwarfs by Gizis *et al.* (in prep.).

3.2. Near-infrared atomic and molecular features

Near-infrared spectra of ultracool dwarfs are dominated by the broad absorption bands at 1.4 and $1.85\mu\text{m}$ due to H_2O . Detailed spectroscopy, however, reveals numerous other features. Early and mid-type M dwarfs exhibit numerous atomic lines, principally in the

J and K windows, due to the alkaline elements (Na, Ca, K), iron, titanium and silicon (Mould, 1978; Kleinmann & Hall, 1986; Davidge & Boeshaar (1991)). Observations of the M8 dwarfs TVLM 513-46546 and Gl 569B by Viti & Jones (1999) show that while the atomic lines remain prominent in the J passband, the longer wavelength features weaken at these later spectral types.

Figures 6, 7 and 8 present J, H and K-band spectra of the eighteen ultracool dwarfs considered here. We have identified the more prominent atomic features, including the two K I doublets, at 1.169/1.177 and 1.244/1.252 μm and the Na I doublet at 1.138/1.140 μm . The last mentioned is unresolved at the resolution of the current spectra, and can be distorted by terrestrial H_2O absorption. An absorption line due to the blended Na I 2.206/2.209 μm doublet is detected in some spectra, while narrow lines, possible due to Al I, are also evident at $\sim 1.3\mu\text{m}$ in LHS 2065 and GD 165B. Table 3 lists measurements of the equivalent widths of these features, including the strongest FeH bandhead (possibly blended with VO) at 1.2 μm . The wings of the KI 1.244/1.252 μm doublet overlap at the resolution of our observations, so we give the joint equivalent width. The uncertainties in the measurements vary, dependent on the signal-to-noise of the individual spectra, but are typically 1 to 2 \AA .

None of the CGS4 spectra show evidence for the 1.71 μm Mg I feature detected in TVLM 513-46546 by Viti & Jones (1999). However, inspection of the spectral sequence in figure 7 suggests the presence of recurrent features near the peak of the H-band flux distribution. Those features are present in both our own observations and the L2001 dataset, and may also be evident in Mould's (1978) observations of Gl 699 and in TVLM 513-46546 (Figure 2 in Viti & Jones, 1999). Figure 9 shows an expanded plot of the region, including four L dwarfs with relatively high signal-to-noise data, and the normalised spectrum of the F6 dwarf, BS1358. Three possible features in the L dwarf spectra, at 1.58, 1.613 and 1.627 μm , are identified; at least the first mentioned also appears to be present in M8 dwarfs. All three are close to, but not exactly coincident with, terrestrial absorption in the BS1358 spectrum. However, the features appear to increase in strength from M8 to L4/L5, declining rapidly to the threshold of detection in the L7 dwarf Denis 0205. This is consistent with an intrinsic origin, and the absorption pattern is suggestive of molecular absorption. Higher resolution, high signal-to-noise spectra at these wavelengths are required to confirm the nature of these features.

The central regions of the near-infrared steam bands are masked by terrestrial absorption, even in observations from Mauna Kea. The higher temperatures in late-M and L dwarf atmospheres, however, lead to broader bands, placing the wings in regions accessible to observation. H_2O absorption increases in strength through spectral type M,

and Martin *et al.* (1999) find that trend to continue through mid-type L dwarfs, at least at $1.4\mu\text{m}$. We have constructed four indices designed to measure the depth of the 1.4 and $1.85\mu\text{m}$ bands. The indices are defined as

$$\begin{aligned} H_2O^A &= \frac{F_{1.34}}{F_{1.29}} & H_2O^B &= \frac{F_{1.48}}{F_{1.60}} \\ H_2O^C &= \frac{F_{1.70}}{F_{1.80}} & H_2O^D &= \frac{F_{2.0}}{F_{2.16}} \end{aligned}$$

In each case, the flux measurement is defined as the average flux in a $0.02\mu\text{m}$ window centred on the wavelength in question; that is, $F_{1.34}$ is the average flux in interval $1.33 < \lambda < 1.35\mu\text{m}$. Note that $F_{1.34}$, in particular, lies in close proximity to a region affected by terrestrial H_2O absorption.

The triple bandheads produced by the first overtone transitions of the CO molecule are also evident at $2.3\mu\text{m}$ in the K passband, with the longer wavelength transitions becoming less distinct with increasing spectral type and barely detectable beyond L5. We have measured a bandstrength for this feature by constructing the R_{CO} index, defined as the ratio between the flux at the base of the primary bandhead (at $2.29\mu\text{m}$) and the pseudo-continuum flux at $2.27\mu\text{m}$. Tokunaga & Kobayashi (1999) have shown that H_2 absorption is also present at $\sim 2.2\mu\text{m}$ in later-type L dwarfs. They define two indices,

$$K1 = \frac{\langle F_{2.10-2.18} \rangle - \langle F_{1.96-2.04} \rangle}{0.5(\langle F_{2.10-2.18} \rangle + \langle F_{1.96-2.04} \rangle)}$$

and

$$K2 = \frac{\langle F_{2.20-2.28} \rangle - \langle F_{2.10-2.18} \rangle}{0.5(\langle F_{2.20-2.28} \rangle + \langle F_{2.10-2.18} \rangle)}$$

$K1$, like H_2O^D , provides a measure of the red wing of the $1.85\mu\text{m}$ steam band, while $K2$ is sensitive to the presence of H_2 absorption.

None of the spectra, including our observations of the L8 dwarf, 2M0310, show evidence for methane absorption in either the H or K band. However, the J-band spectrum of 2M0825 clearly shows the onset of broad H_2O absorption at 1.1 to $1.2\mu\text{m}$, a prominent feature in the early-type T dwarfs discovered by Leggett *et al.* (2000). Table 4 lists the molecular indices for the eighteen ultracool dwarfs in the current sample. The measured ratios are typically uncertain to $\pm 5\%$.

3.3. Spectral type calibration at near-infrared wavelengths

Figure 10 plots the variation with spectral type of the equivalent widths of the atomic sodium and potassium lines present in the J-band. In both this figure and the succeeding

figures, we represent spectral type numerically, setting $-2 \equiv M8$, $0 \equiv L0$, $5 \equiv L5$ and so forth. All of the equivalent widths show significant dispersion at a given spectral type, at least partially due to the measurement uncertainties. The potassium lines reach maximum strength at type L3/L4, and decline rapidly at later types. The sodium blend increases in strength from M8 to L5, but is ill defined at later spectral types. We note also that the $2.20 \mu\text{m}$ Na I line is not detected in most mid-type L dwarfs, but appears to be present in 2M0036 and Denis 0205. It is not clear whether this is an intrinsic effect or more a reflection of signal-to-noise in the various spectra.

Of the molecular indices, the R_{CO} ratio is essentially unchanged over the full spectral range. In similar fashion, most dwarfs show little evidence for H_2 absorption. The upper panel of Figure 11 plots Tokunaga & Kobayashi’s (1999) K1 and K2 indices; as pointed out by those authors, Denis 0205 stands out from the main body, with a significantly-depressed K2 index. 2M0310 lies even further below the mean, although the L7.5 dwarf, 2M0825, is unremarkable in this diagram. Inspection of the K-band spectra plotted in Figure 8 suggests substantial H_2 absorption is present in 2M0310.

The lower panel in Figure 11 plots the K1 index against optical spectral type. The data are well correlated for spectral types earlier than L6, and least-squares fitting gives the relation

$$Sp = (-2.8 \pm 0.6) + (21.8 \pm 2.8)K1, \quad \sigma = \pm 0.95$$

Figure 12 plots the four H_2O indices defined in the previous section. All are well correlated with optical spectral type, although both H_2O^A and H_2O^D “saturate” at later spectral types. H_2O^A and H_2O^B show the least dispersion, with

$$Sp = 23.4 \pm 2.7 - (32.1 \pm 4.2)H_2O^A, \quad \sigma = \pm 1.18$$

where the fit is valid for spectral types earlier than L6, and

$$Sp = 20.7 \pm 1.6 - (24.9 \pm 2.2)H_2O^B, \quad \sigma = \pm 1.02$$

for spectral types M8 to L8. Combined with the K1 calibration given above, these relations bridge the optical/infrared divide; infrared spectroscopy can be used to determine spectral types consistent with optically-defined K99 system.

4. Summary and conclusions

We have presented near-infrared spectra for a sample of eleven ultracool dwarfs. Our observations complement the dataset compiled previously by Leggett *et al.* (2001),

providing good coverage of optically-defined spectral types from M8 to L8. We have combined these near-infrared data with optical spectra, integrating the energy distribution to derive bolometric magnitudes. Our results confirm previous suggestions that there is relatively little variation in the J-band bolometric correction for cool dwarfs ranging from spectral type \approx M6 to type T (Gl 229B).

Combining the two datasets, we have measured equivalent widths for the stronger atomic lines due to potassium and sodium. The results show that the variation of spectral features between 1 and $2.5\mu\text{m}$ is consistent with the behaviour at far-red wavelengths; specifically, we can map the infrared variation onto the Kirkpatrick *et al.* (1999) spectral classification scheme. The majority of the atomic lines show similar characteristics, increasing in equivalent width to maximum at L3/L4, with a more rapid decline in strength at longer wavelengths. The exception is the $2.2\mu\text{m}$ Na I line, although its intermittent detection may simply reflect the signal-to-noise of the observations. Inspection of the combined suite of near-infrared spectra suggests that there are intrinsic absorption features between 1.58 and $1.63\mu\text{m}$ which remain to be identified.

Besides measuring equivalent widths for atomic lines, we have constructed narrowband indices designed to measure the strength of the prominent molecular absorption bands due to water and CO. Even the latest-type dwarf observed, spectral type L8, shows no evidence for methane absorption. There is little variation in CO absorption, but all four H_2O indices exhibit a good correlation with spectral type, with the best calibration provided by H_2O^B , measuring the depth of absorption in the redward wing of the $1.4\mu\text{m}$ steam band.

Our analysis is based on the most extensive set of near-infrared spectra currently available. Even so, we have data for only fourteen L dwarfs, four of which have incomplete spectral coverage. Observations of a larger sample of ultracool dwarfs are required to verify these results. However, the correlations derived here not only permit extension of the K99 spectral sequence to near-infrared wavelengths, but also indicate that spectral type on that system is monotonically correlated with changes in the effective temperature of these low-mass dwarfs.

We would like to thank Thor Wald and Tom Kerr for assistance in obtaining our observations and with the initial data reduction. We also thank Sandy Leggett for making the L2001 spectra readily available in electronic form. INR and JDK acknowledge partial support from a NASA/JPL grant to 2MASS Core Project Science. JEG and JDK acknowledge the support of the Jet Propulsion Laboratory, California Institute of Technology, which is operated under contract with NASA. The United Kingdom Infrared Telescope is operated by the Joint Astronomy Centre on behalf of the Particle Physics and

Astronomy Research Council.

REFERENCES

- Becklin, E.E., Zuckerman, B. 1988, *Nature*, 336, 656
- Boeshaar, P. C. 1976, Ph. d. thesis,
- Dahn, C.C., Guetter, H.H., Harris, H.C., et al., 2000, in *From Giant Planets to Cool Stars*, ASP Conf. Ser. Vol. 212, 74, (ed. Caitlin A. Griffiths & Mark S. Marley)
- Davidge, T.J., Boeshaar, P.C. 1991, *AJ*, 102, 267
- Jones, H.R.A., Longmore, A.J., Allard, F., Hauschildt, P.H. 1996, *MNRAS*, 280, 77
- Kirkpatrick, J.D., Henry, T.J., McCarthy, D.W., Jr. 1991, *ApJS*, 77, 417
- Kirkpatrick, J.D., Henry, T.J., Liebert, J. 1993, *ApJ*, 406, 701
- Kirkpatrick, J.D., Beichman, C.A., Skrutskie, M.F. 1997, *ApJ*, 476, 311
- Kirkpatrick, J.D., Reid, I.N., Liebert, J., Cutri, R., et al. 1999, *ApJ*, 519, 802
- Kirkpatrick, J.D., Reid, I.N., Liebert, J., Gizis, J.E., et al. 2000, *AJ*, 120, 447
- Kleinmann, S.G., Hall, D.N.B. 1986, *ApJS*, 62, 501
- Leggett, S.K., Harris, H.C. 1994, *AJ*, 108, 944
- Leggett, S.K., Toomey, D.W., Geballe, T.R., Brown, R.H. 1999, *ApJ*, 517, L139
- Leggett, S.K., Geballe, T.R., Fan, X. et al. 2000, *ApJ*, 536, L35
- Leggett, S.K., Allard, F., Geballe, T.R., Hauschildt, P.H., Schweitzer, A. 2001, *ApJ*, in press
- McLean, I.S., Wilcox, M.K., Becklin, E.E. et al. 2000, *ApJ*, 533, L45
- Martin, E.L., Delfosse, X., Basri, G., Goldman, B., Forveille, T., Zapatero Osorio, M.R. 1999, *AJ*, 118, 2466
- Mould, J.R. 1978, *ApJ*, 226, 923
- Morgan, W.W., Keenan, P.C., Kellman, E. 1943, *Atlas of Stellar Spectra*, Univ. of Chicago Press, Chicago
- Nakajima, T., Durrance, S.T., Golimowski, D.A., Kulkarni, S.R. 1994, *ApJ*, 428, 797
- Oke, J. B., Cohen, J. G., Carr, M., Cromer, J., et al. 1995, *PASP*, 107, 375
- Reid, I.N., Gizis, J.E., Kirkpatrick, J.D., Koerner, D.W. 2000, *AJ*, in press
- Secchi, A., 1866, *Comptes Rendu*, 63, 621

Tinney, C.G. 1993, AJ, 105, 1169

Tinney, C.G., Delfosse, X., Forveille, T., Allard, F. 1998, A&A, 338, 1066

Tokunaga, A., Kobayashi, N. 1999, AJ, 117, 1010

Viti, S., Jones, H.R.A. 1999, A&A, 351, 1028

Table 1: Observing Log

2MASS	Sp.	J	J-K _S	J1	J2	H	K	reference
IJ0429028+133759	M7	12.67	1.03	960s	960s	960s	960s	HR 1358, F6
WJ0320596+185423	M8	11.74	1.17	960	960	640	960	HR 869, F6
PJ0345432+254023	L0	14.03	1.33	2880	2880	2880	1920	HR 1238, F4
WJ0746425+200032	L0.5	11.74	1.25	960	960	640	1280	HR 2835, F6
WJ0829066+145622	L2	14.72	1.60		2400	1920	1280	HR 3299, F6
IJ1029216+162652	L2.5	14.31	1.70		1440	960	960	HR 3998, F7
WJ0036159+182110	L3.5	12.44	1.41	960	960	960	1280	HR 217, F8
IJ1112256+354813	L4.5	14.57	1.77		1600	1600	1280	HR 4412, F7
DENIS-P J0205.4-1159	L7	14.55	1.56	3840	3840	2240	1280	HR 638, F5
WJ0825196+211552	L7.5	15.12	2.07	3840	3840	2240	2560	HR 3299, F6
WJ0310599+164816	L8	16.43	2.03		4320	2240	1920	HR 869, F6

Notes: Columns 3 and 4 list near-infrared photometry from 2MASS.

Columns 5 to 8 list the total integration time (in seconds) for each of the four wavelength ranges described in the text.

Column 9 identifies the reference star used to calibrate each target.

2MASS IJ0429028+133759 is LP 475-855 (Leggett & Harris, 1994)

2MASS WJ0320596+185423 is the proper motion star LP 412-31

2MASS IJ1112256+354813 is also known as Gl 417B

Table 2: Photometric properties

Name	Sp. type	J	(I-J)	(J-H)	(H-K _s)	BC _J	π (mas)	source
2M0320/LP412-31	M8	11.74	3.05	0.71	0.51	1.97	68.0±0.7	USNO
TVLM 513-46546	M8.5	11.80	3.41	0.68	0.40	2.05	94.3±0.7	USNO
LHS 2065	M9	11.22	3.22	0.80	0.48	1.90	117±2	L2001
BRI0021-0214	M9.5	11.80	3.39	0.76	0.46	1.95	82 ± 2 ^C	L2001
2M0345	L0	13.92	3.44	0.76	0.54	2.01	36.7 ± 0.7	USNO
2M0746 ^A	L0.5	11.73	3.38	0.77	0.47	2.01	82.6 ± 2	USNO
2M0829	L2	14.72		0.93	0.67	1.66		2MASS
2M1029	L2	14.31		0.96	0.74	1.92		2MASS
Kelu 1 ^B	L2	13.42	3.52	0.95	0.67	1.67	52.1 ± 2.0	USNO
Denis 1058	L3	14.16	3.64	0.88	0.63	1.76	57.0 ± 1.2	USNO
2M0036	L3.5	12.44	3.67	0.84	0.54	1.99	112.4 ± 2.0	USNO
GD 165B	L4	15.71	3.45	1.03	0.55	1.69	31 ± 2	L2001
2M1112 ^B	L4.5	14.57		1.10	0.78	1.61	46.0±0.8 ^D	2MASS
Denis 1228 ^{A,B}	L5	14.37	3.84	0.97	0.66	1.66	51 ± 3	USNO
SDSS 0539	L5	13.94	3.73	0.97	0.53	1.76		L2001
Denis 0205 ^A	L7	14.59	3.85	0.97	0.56	1.71	55.5 ± 2.3	USNO
2M0825 ^B	L7.5	14.99	4.23	1.17	0.80	1.70		USNO
2M0310 ^B	L8	16.43		2.03	1.48	1.66		2MASS

Source: USNO - IJHK Dahn *et al.* (2000)

2MASS - I, Dahn *et al.* (2000); JHK_S, 2MASS

L2001 - IJHK, Leggett *et al.* (2001)

Notes:

- A. known L-dwarf/L-dwarf binary
- B. Li 6708Å detection implies $M \leq 0.06M_{\odot}$
- C. Parallax from Tinney (1996)
- D. Parallax from Hipparcos astrometry of Gl 417A

Table 3: Equivalent width measurements

Name	Sp. type	Na I	Na I	K I	K I	K I	FeH
		1.14 μ m	2.2 μ m	1.169 μ m	1.197 μ m	1.24/1.25 μ m	1.2 μ m
LP 412-31	M8	20.2	10.1	5.7	6.6	17.8	16.3
TVLM 513-46546	M8.5	21.5	3.3	6.4	8.6	22.6	19.0
LHS 2065	M9	18.7	3.0	6.2	7.5	19.0	18.3
BRI0021-0214	M9.5	20.8	5.7	5.4	7.1	21.8	22.6
2M0345	L0	14.8		9.5	8.8	21.0	18.8
2M0746	L0.5	19.4		7.8	10.5	23.6	19.2
2M0829	L2	16.1		6.8	9.3	25.6	23.0
2M1029	L2					24.2	
Kelu 1	L2	22.4		8.8	8.9	25.3	20.1
Denis 1058	L3	23.5		10.8	16	46.8	27.2
2M0036	L3.5	27.3	3.4	10.9	14.0	37.4	23.1
GD 165B	L4	32.2		8.3	9.8	28.6	19.0
2M1112	L4.5					29.9	
Denis 1228	L5	20.7		7.1	10.1	20.9	16.7
SDSS 0539	L5	23.9		9.2	11.3	22.9	18.6
Denis 0205	L7	24.8	3.9	8.6	8.3	16.8	
2M0825	L7.5		8.2	4.8	4.2	8.5	
2M0310	L8		10:			9.0	

Equivalent widths given in Ångstroms.

Table 4: Molecular band indices

Name	Sp. type	H_2O^A	H_2O^B	H_2O^C	H_2O^D	K1	K2	R_{CO}
LP 412-31	M8	0.79	0.91	0.71	0.96	0.03	-0.09	0.77
TVLM 513-46546	M8.5	0.71	0.87	0.64	0.89	0.10	-0.03	0.82
LHS 2065	M9	0.77	0.88	0.71	0.88	0.11	-0.01	0.82
BRI0021-0214	M9.5	0.70	0.82	0.66	0.82	0.16	-0.01	0.80
2M0345	L0	0.72	0.81	0.69	0.94	0.08	-0.03	0.75
2M0746	L0.5	0.68	0.79	0.63	0.87	0.12	-0.08	0.77
2M0829	L2	0.72	0.79	0.73	0.72	0.28	0.03	0.74
2M1029	L2	0.64	0.71	0.70	0.74	0.26	-0.03	0.72
Kelu 1	L2	0.65	0.71	0.61	0.74	0.26	-0.01	0.78
Denis 1058	L3	0.63	0.67	0.65	0.78	0.17	-0.01	0.81
2M0036	L3.5	0.57	0.66	0.54	0.74	0.26	-0.08	0.77
GD 165B	L4	0.61	0.72	0.55	0.73	0.30	-0.04	0.76
2M1112	L4.5	0.64	0.62	0.59	0.69	0.32	-0.10	0.75
Denis 1228	L5	0.63	0.67	0.65	0.78	0.32	-0.08	0.77
SDSS 0539	L5	0.54	0.65	0.51	0.71	0.32	-0.09	0.80
Denis 0205	L7	0.56	0.57	0.46	0.70	0.34	-0.16	0.79
2M0825	L7.5	0.62	0.64	0.63	0.69	0.33	-0.08	0.75
2M0310	L8	0.51	0.46	0.48	0.77	0.26	-0.26	0.76

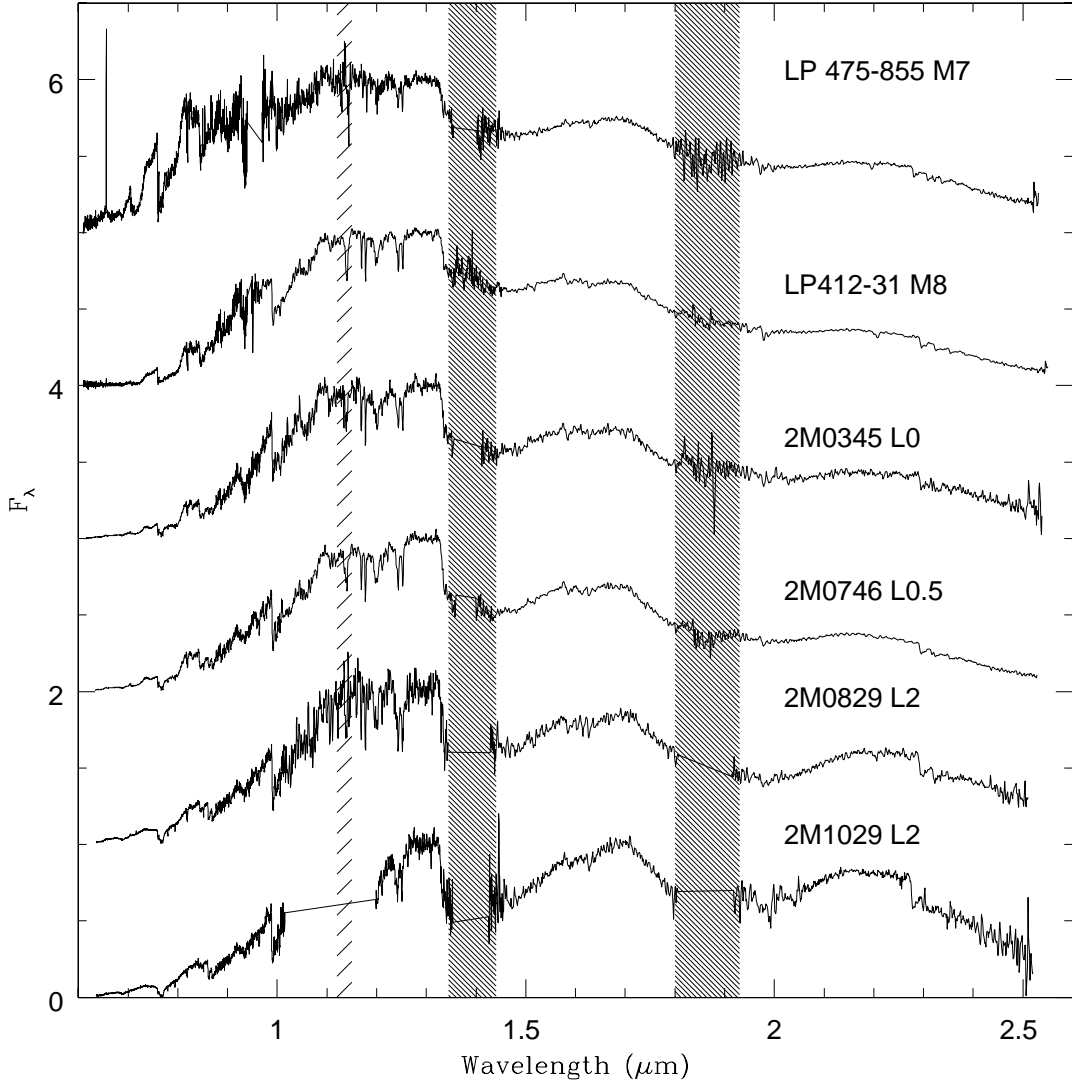


Fig. 1.— Optical and near-infrared spectra of the earlier-type dwarfs in the present sample. All of the spectra are normalised to the mean flux at $1.28 \pm 0.01 \mu\text{m}$ and the shaded regions denote wavelengths affected by terrestrial water vapour absorption; the lighter-shaded $1.14\mu\text{m}$ band is significantly weaker than the 1.4 and $1.85\mu\text{m}$ absorption. The optical data are from our Keck LRIS observations with the exception of LP 475-855, which was observed using the Modular Spectrograph on the Du Pont 100-inch at Las Campanas observatory. The last-mentioned star was caught during a flare outburst, accounting for the strong emission at H α .

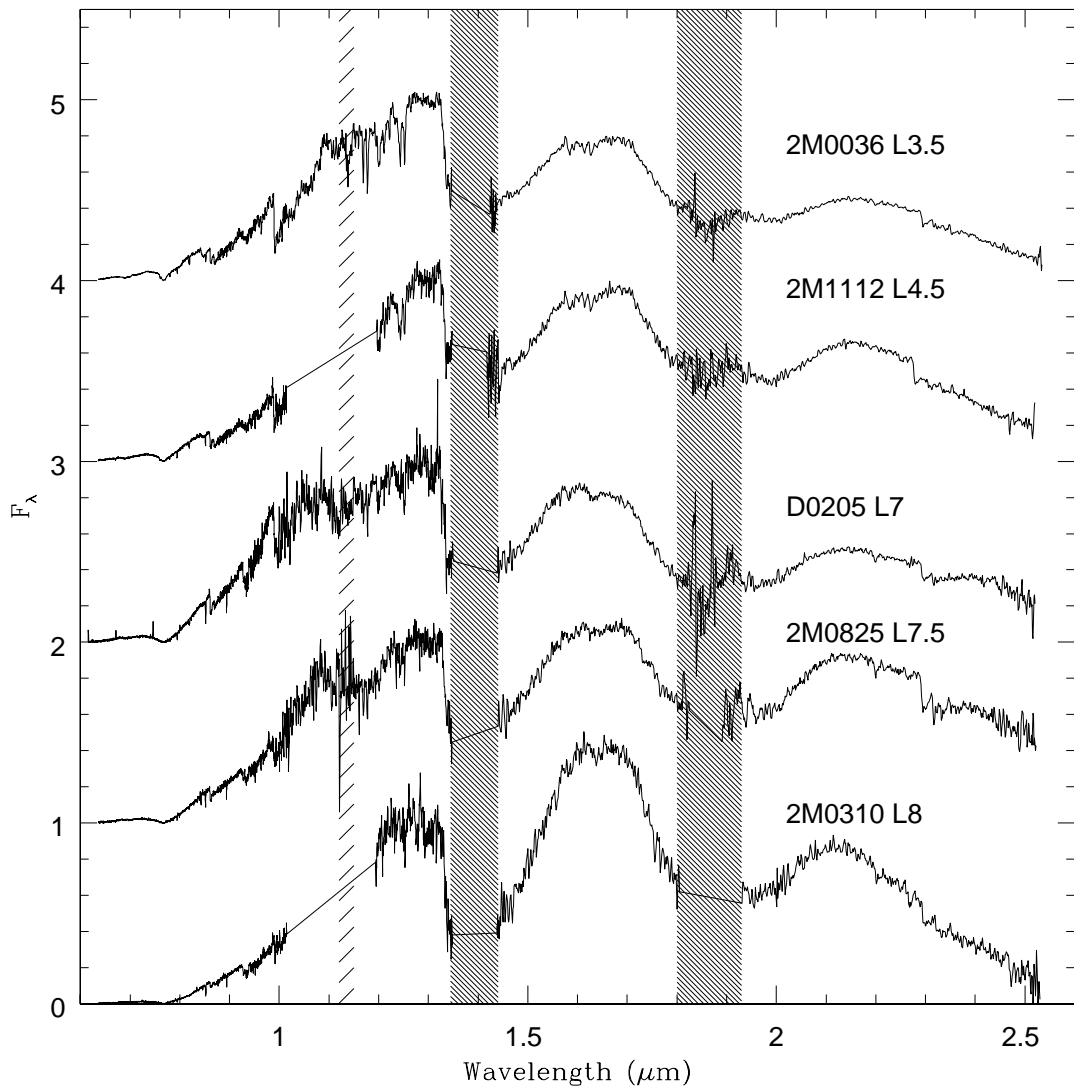


Fig. 2.— Optical and near-infrared spectra of the later-type dwarfs in the present sample.

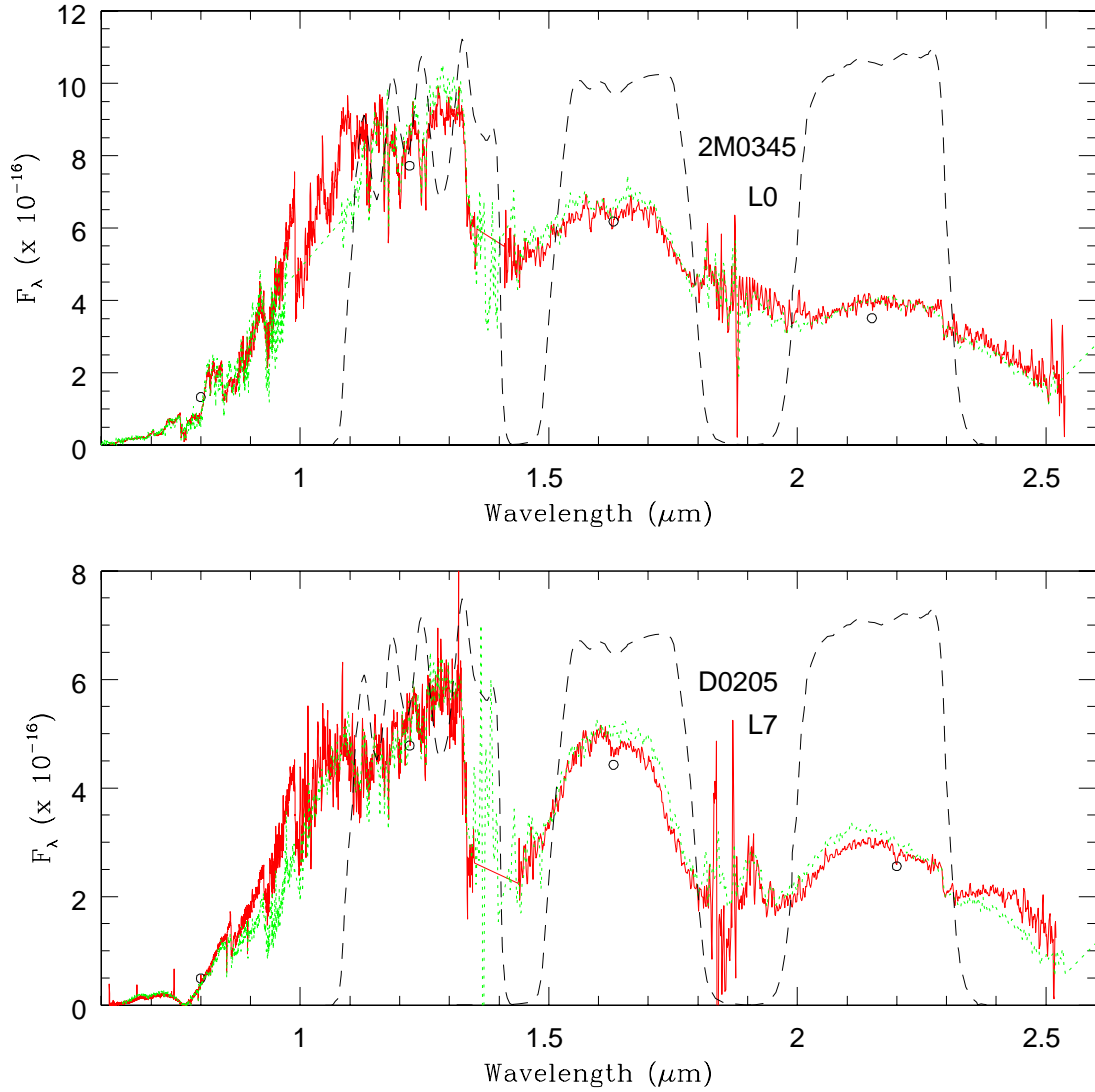


Fig. 3.— Comparison between our observations of 2M0345 and Denis 0205 and the near-infrared spectroscopy of Leggett *et al.* (2001). Our data are plotted as a solid line. The 2MASS JHK_s photometric passbands are superimposed on the data.

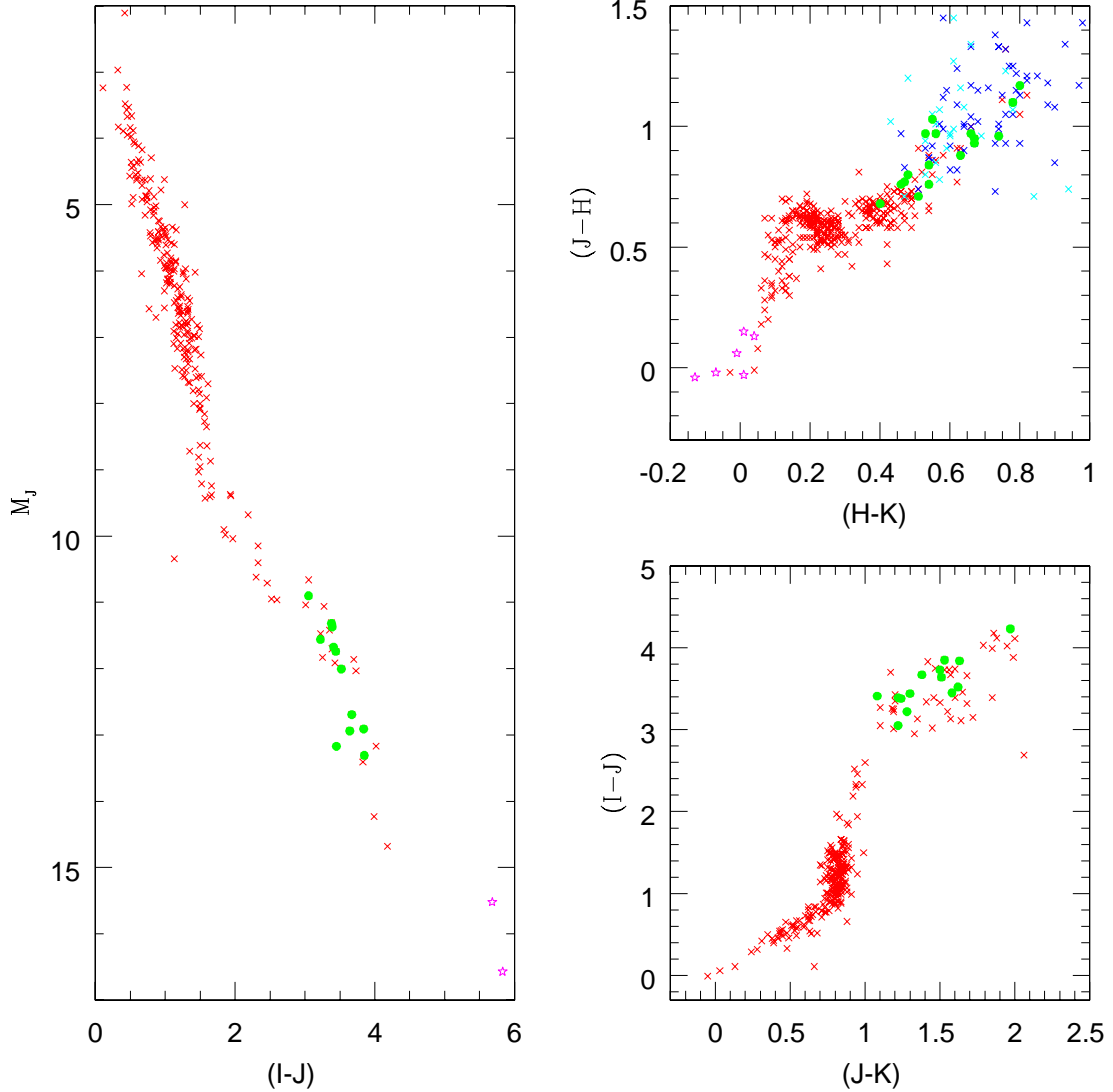


Fig. 4.— Colour-magnitude and colour-colour data for late-type dwarfs. The solid points identify the ultracool dwarfs with CGS4 near-infrared data - the sources listed in Table 2. Crosses are nearby stars (photometry from Leggett, 1992) and L dwarfs, from Kirkpatrick *et al.* (1999, 2000); five-point stars are T dwarfs.

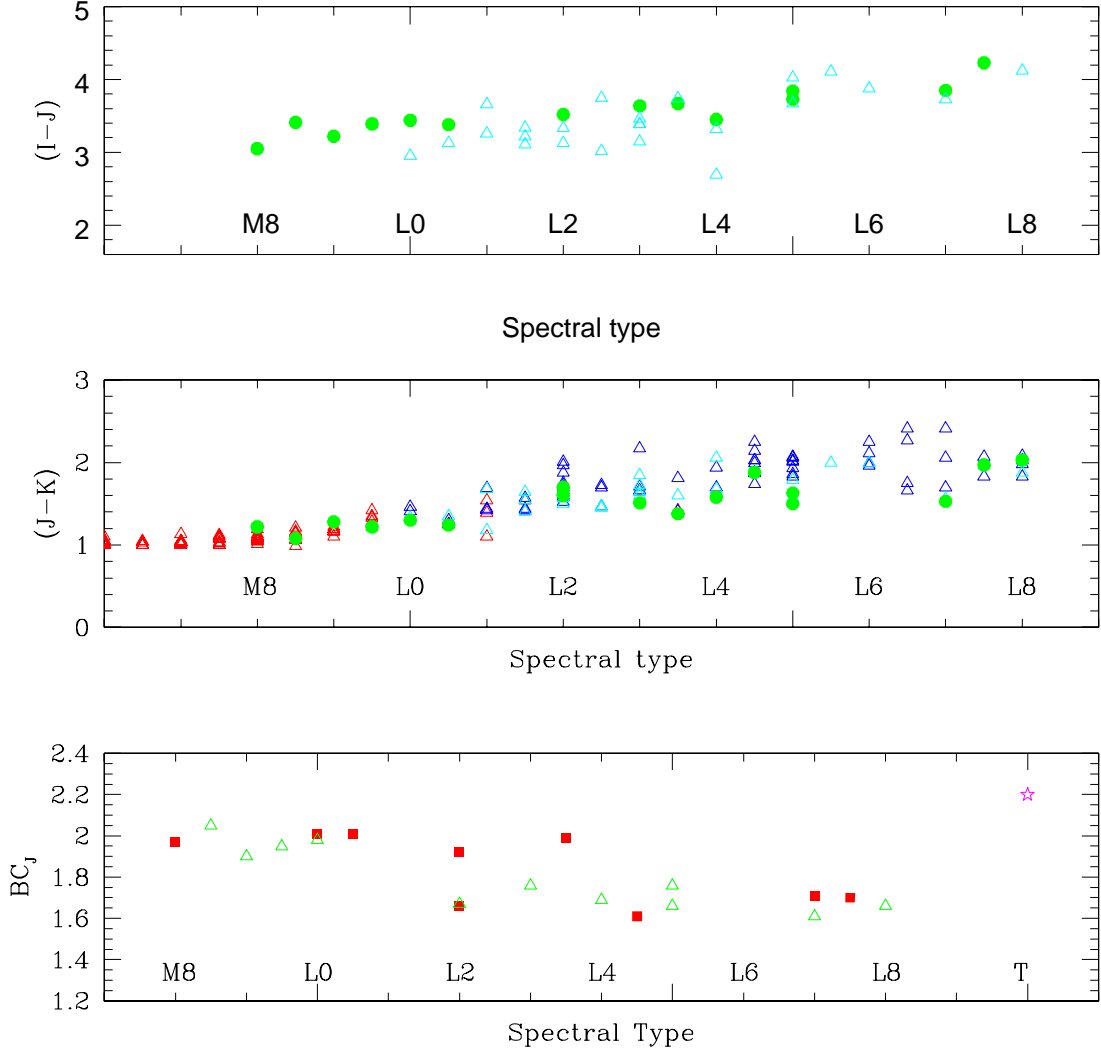


Fig. 5.— Colour/spectral-type relations for ultracool dwarfs. In the upper two panels, open triangles are L dwarfs from Kirkpatrick *et al.* (1999, 2000); solid points plot data for the dwarfs listed in Table 2. The lowest panel plots the J-band bolometric correction as a function of spectral type, where the solid squares are from our analysis, while the open triangles are taken from the L2001 calibration. The five-point star marks Gl 229B.

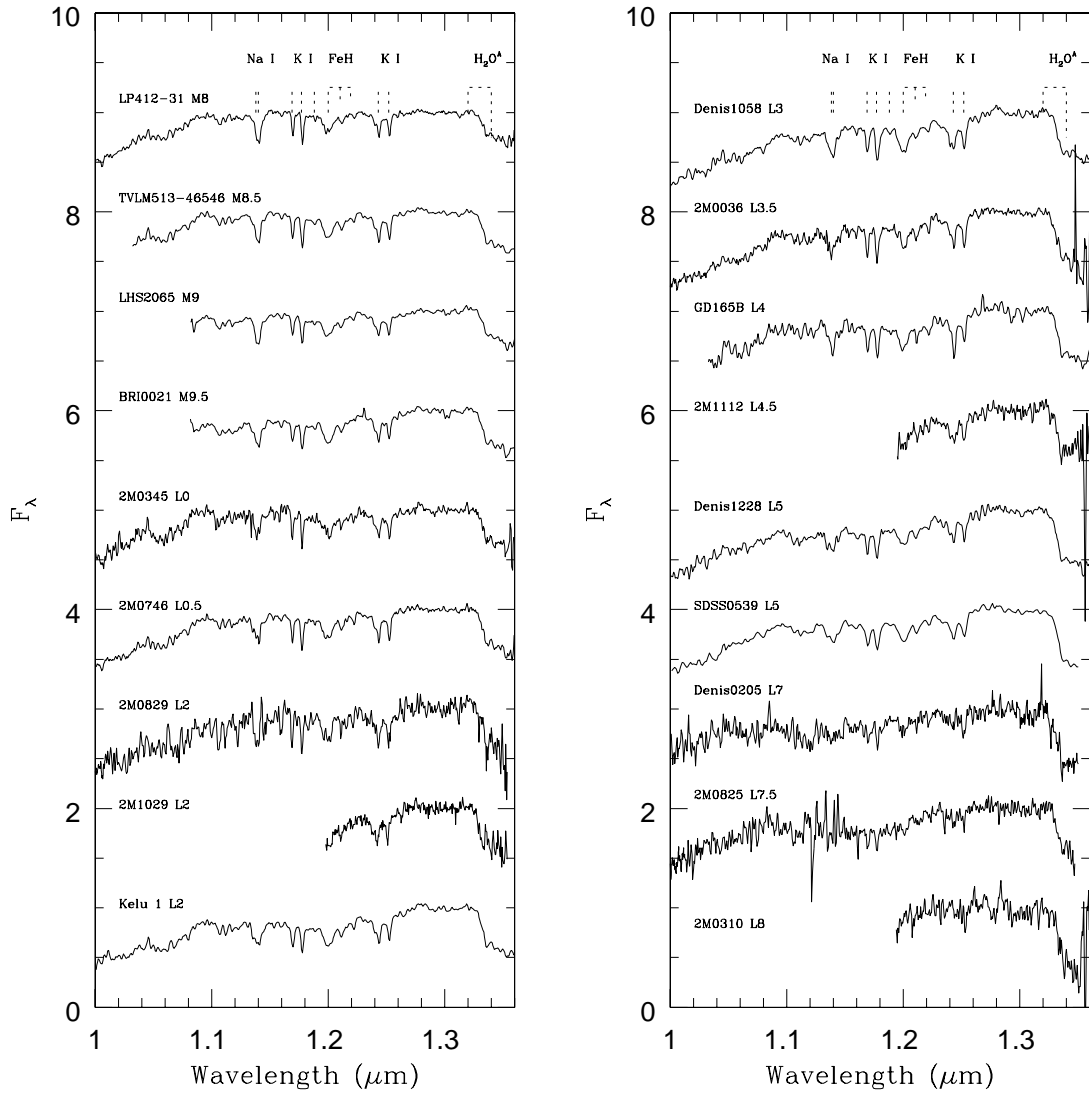


Fig. 6.— J-band spectra of the 18 ultracool dwarfs from L2001 and our own observations. The more prominent atomic and molecular features are identified.

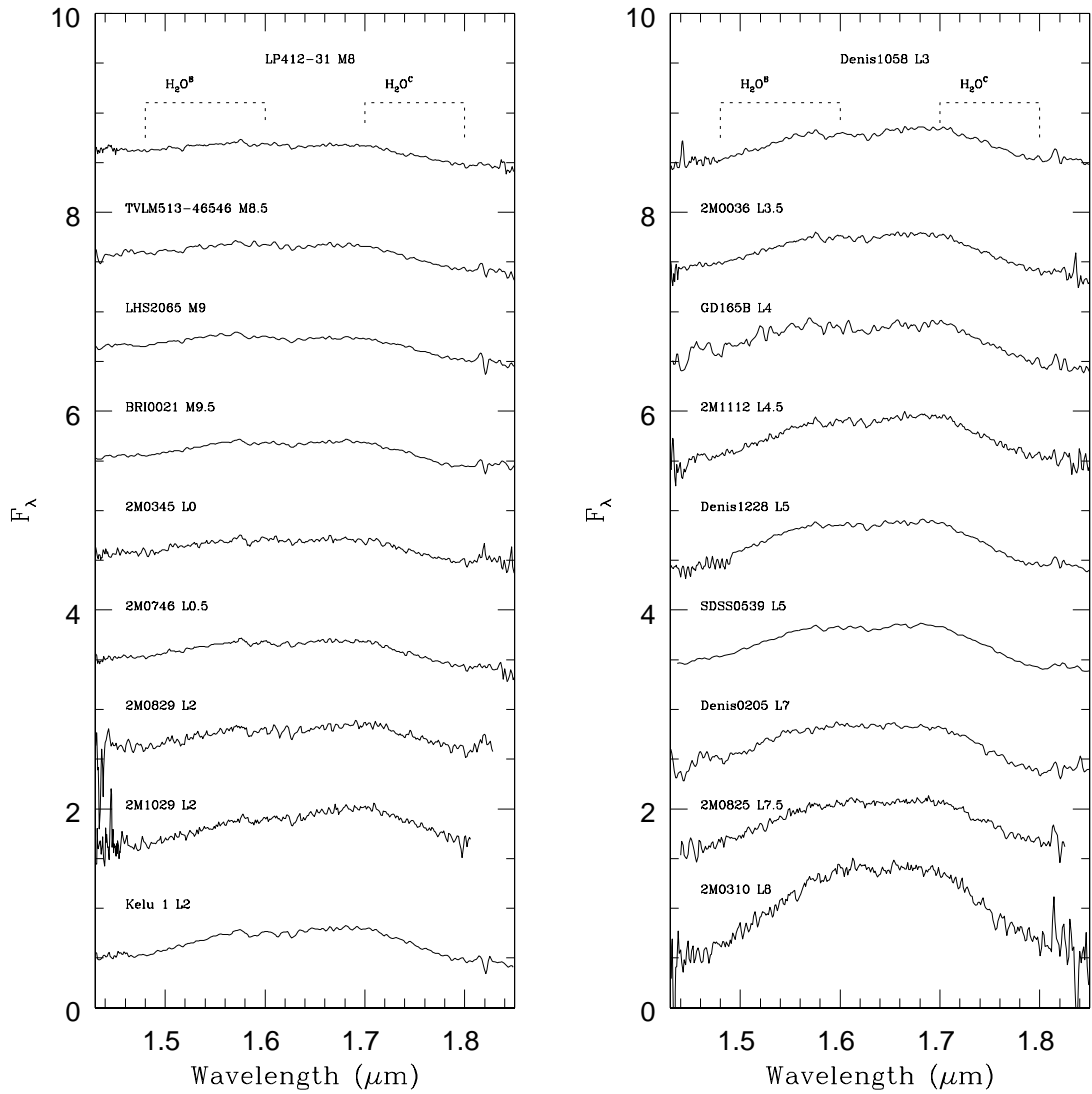


Fig. 7.— H-band spectra of the 18 ultracool dwarfs from L2001 and our own observations.

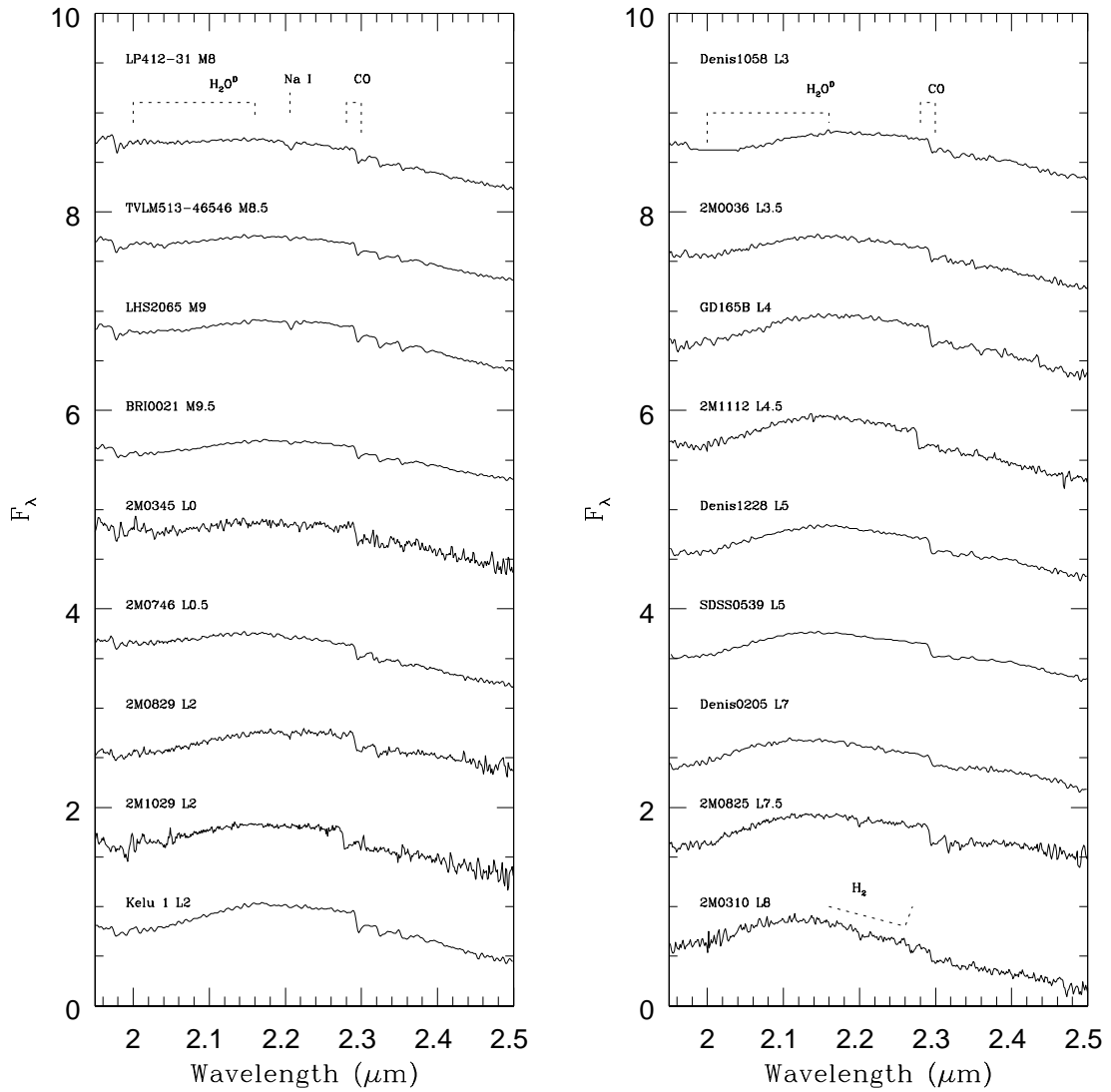


Fig. 8.— K-band spectra of the 18 ultracool dwarfs from L2001 and our own observations.

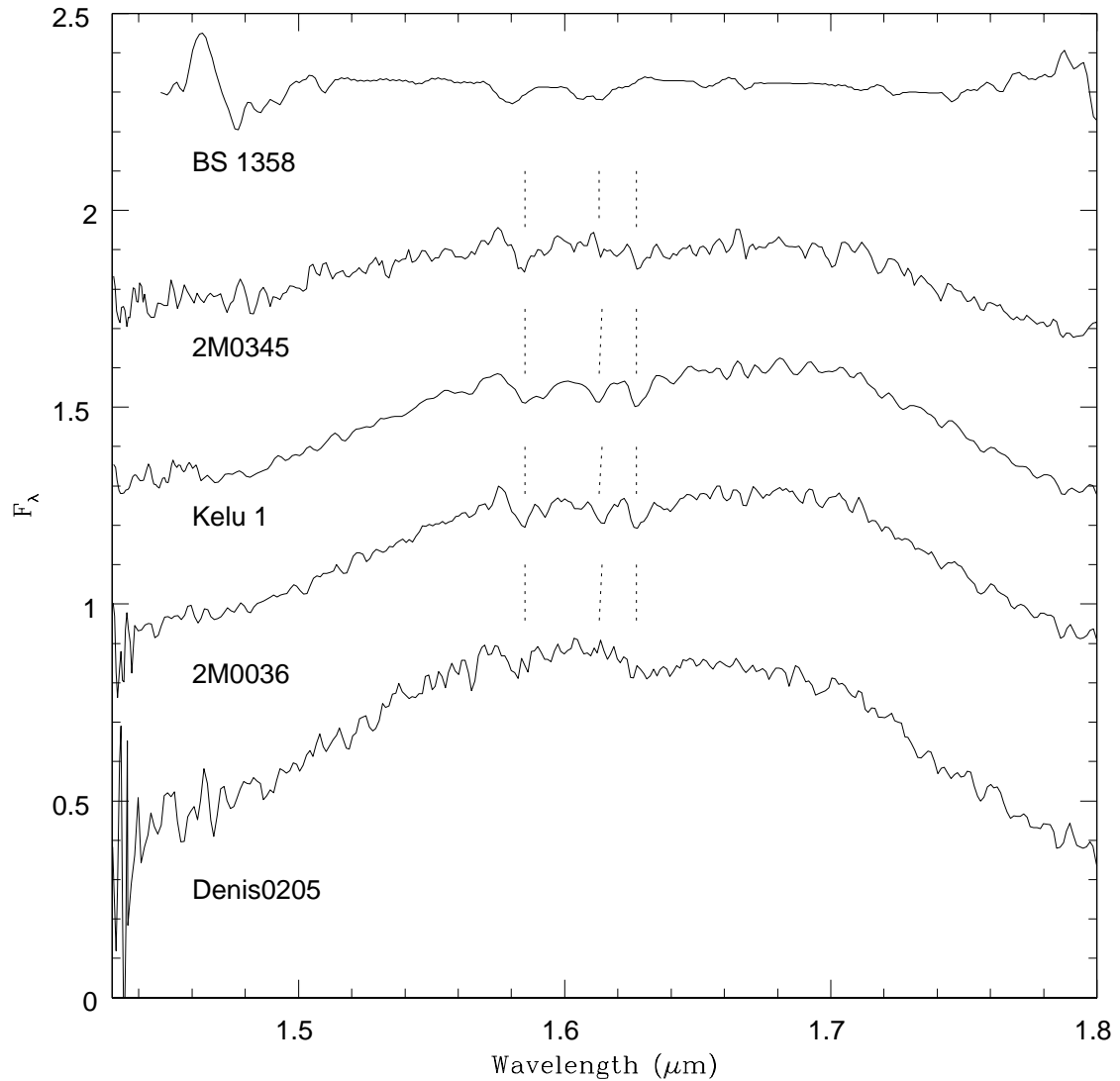


Fig. 9.— An expanded plot of the H-band region in four L dwarfs, 2M0345 (L0), Kelu 1 (L2), 2M0036 (L3.5) and Denis0205 (L7). The possible atomic or molecular features discussed in the text are marked, and the normalised spectrum of BS 1358 plotted for comparison. The “feature” at $1.4\mu\text{m}$ in the standard star spectrum is a product of the continuum fitting, and does not affect calibration of the program objects.

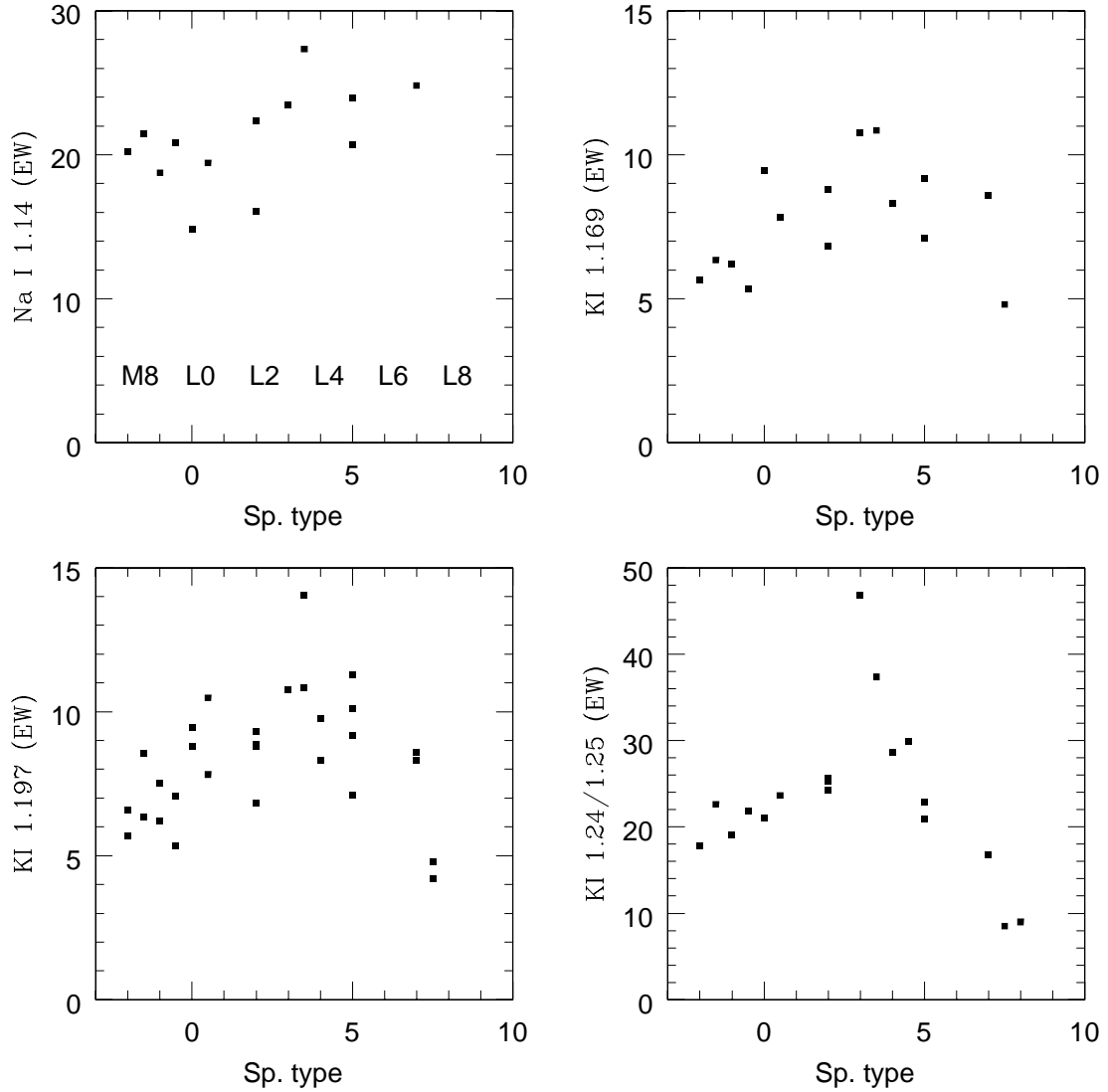


Fig. 10.— The variation in equivalent width of the Na I and K I doublets as a function of spectral type. As noted in the text, we represent spectral type numerically with $M8 \equiv -2$, $L0 \equiv 0$ and $L5 \equiv 5$. The equivalent widths are measured in Ångstroms.

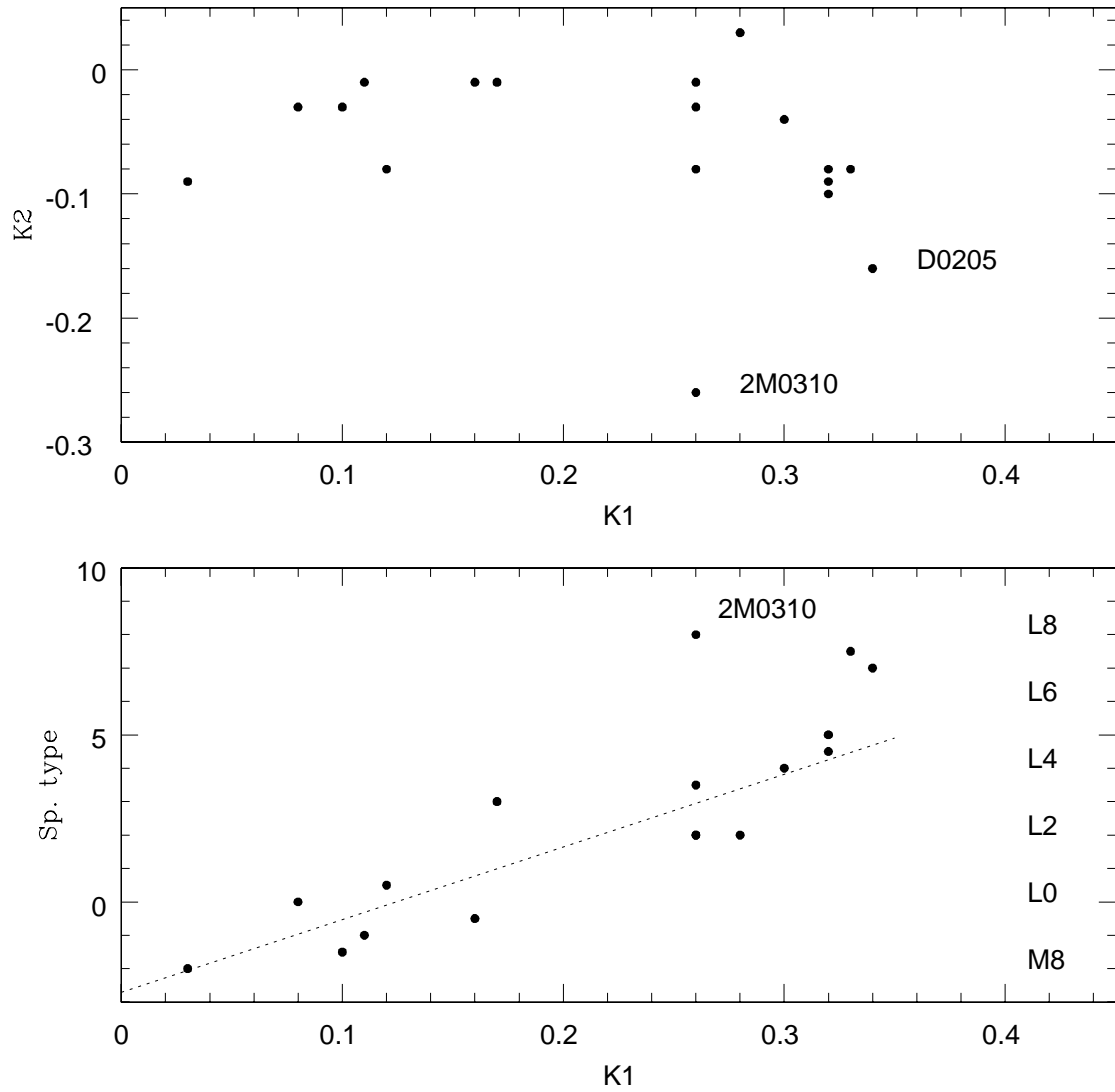


Fig. 11.— The K1 and K2 indices defined by Tokunaga & Kobayashi (1999). K2 provides a measure of H_2 absorption, and the upper panel shows that Denis 0205 and 2M0310 stand out in the present sample. The lower panel shows that K1 is well correlated with optical spectral type for dwarfs earlier than L6; the dotted line shows the linear fit to the data cited in the text.

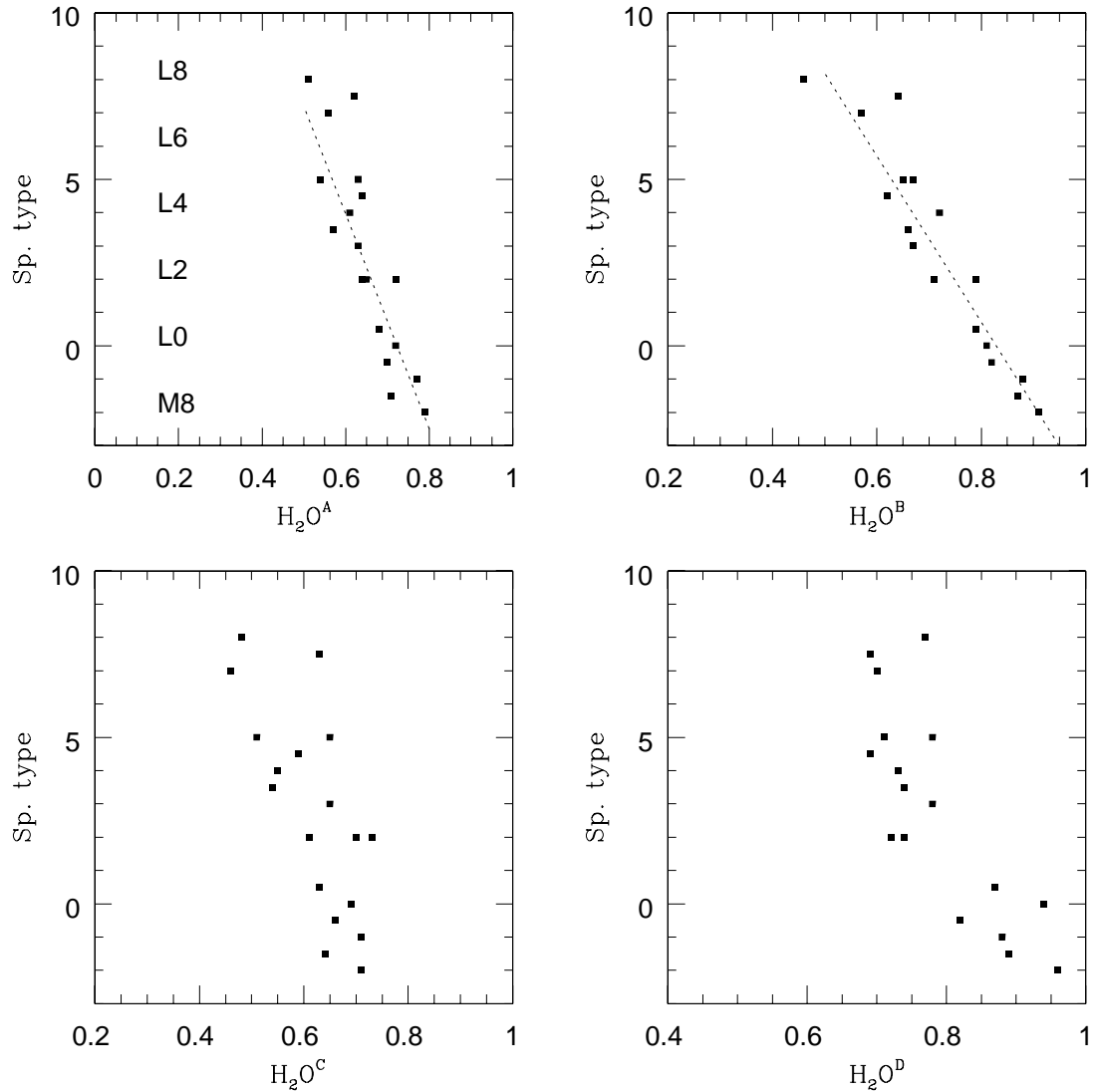


Fig. 12.— Spectral type as a function of H_2O bandstrength. The dotted lines plotted in the upper two panels are the linear calibrations listed in the text.